

A Test on Different Types of the Time Curve of Hardness Ratio of Gamma-Ray Bursts based on the Curvature Effect *

Lan-Wei Jia

National Astronomical Observatories/ Yunnan Observatory, Chinese Academy of Sciences, Kunming 650011, China; lwjia@ynao.ac.cn
Graduate School of Chinese Academy of Sciences, Beijing 100049, China

Received 2007 September 21; accepted 2007 November 19

Abstract We analyzed a sample of 66 gamma-ray bursts (GRBs) and statistically confirmed the prediction on the time curve of the hardness ratio of GRBs made by Qin et al. based on the curvature effect. In their analysis, GRB pulses are divided into three types according to the shape of their raw hardness ratio (RHR) time curves, defined as to include the background counts to the signal counts, so as to make use of counts within small time intervals. Of the three types, very hard sources exhibit a perfect pulse-like profile (type 1), hard bursts possess a pulse-like profile with a dip in the decay phase (type 2), and soft bursts show no pulse-like profile but have only a dipped profile (type 3). In terms of the conventional hardness ratio, type 3 sources are indeed generally softer than those of type 1 and type 2, in agreement with the prediction. We found that the minimum value of RHR is sensitive in distinguishing the different types. We propose that GRB pulses can be classified according to the minimum value of RHR and that the different type sources may be connected with different strengths of the shock or/and the magnetic field.

Key words: gamma-rays: bursts — gamma-rays: observations — methods: statistical

1 INTRODUCTION

Properties of GRB afterglow have been well studied during the past few years especially after the launch of the Swift satellite (Gehrels et al. 2004; Barthelmy et al. 2005; Burrows et al. 2005; Fox et al. 2005; Gehrels et al. 2005; Tagliaferri et al. 2005; Cusumano et al. 2006; Roming et al. 2006). Probably due to lack of the data in the lower energy bands, the emission processes in the prompt phase of bursts remain unclear.

GRBs are believed to undergo a stage of fireballs which expands relativistically due to the large amount of energy released from them (Goodman 1986; Paczynski 1986). In the case of spherical expansion, Doppler effect over the whole fireball surface would play an important role in producing the spectra of the bursts, observed by a distant observer (see, e.g., Meszaros & Rees 1998; Hailey, Harrison & Mori 1999; Qin 2002, 2003).

A softening of the spectra with time as a general phenomenon, the so-called hard-to-soft phenomenon, was found in early studies of the spectral evolution of GRBs (e.g. Norris et al. 1986). The spectral behaviors of GRB pulses were investigated recently by different group of authors (Kargatis et al. 1995; Ryde & Svensson 2000, 2002; Borgonovo & Ryde 2001; Ryde & Petrosian 2002; Qin et al. 2006; Lu et al. 2007). In interpreting the spectral properties of GRB pulses, the so-called curvature effect is an important factor to be concerned. The curvature effect takes into account the delay of arrival time for photons emitted from different areas of the fireball surface, the growing radius of the fireball, and the shifting spectrum due to the

* Supported by the National Natural Science Foundation of China.

Doppler effect (for detailed explanation, see the introduction in Qin et al. 2006; for a thorough consideration of the effect see Qin 2002). Indeed, the temporal properties of many GRB pulses were found to be well explained by the curvature effect (Fenimore et al. 1996; Ryde & Petrosian 2002; Kocevski et al. 2003; Qin et al. 2004; Qin & Lu 2005).

In revealing the properties of the emission, time-resolved spectra are particularly important. To study the evolution of the hardness of the spectrum of bursts during the period of their pulses, Qin et al. (2006) introduced the so-called “raw hardness ratio” (RHR). The raw hardness ratio is defined as the count of a higher energy channel divided by that of a lower energy channel, where certain background counts are added to the signal counts so that the hardness ratio can be defined within small time intervals. By doing that, one can examine how the hardness varies along with the light curve. In their study, they found that, due to the curvature effect, the peak of the evolutionary curve of the raw hardness ratio would appear in advance of the peak of the light curve.

There are three types of evolutionary curves of RHR, with each type corresponding to a certain form of the RHR profile. The first type arises from a very hard spectrum, the second is associated with a hard spectrum, and the third comes from bursts with soft spectra.

Qin et al. (2006) gave a detailed theoretical analysis but they studied only few GRBs. To check their predictions, we need a statistical study with larger samples. In this paper, we investigate this issue by adopting a GRB sample that comprises a sufficient number of sources. This paper is organized as follows. In Section 2, we describe the sample and the fitting function, in Section 3 we present the results of our analysis, and our conclusions are given in the last section.

2 SAMPLE AND FITTING FUNCTION

Qin et al. (2006) studied the time curve of the hardness ratio of gamma-ray burst pulses due to the Doppler effect and the time delay of the emission from a relativistically expanding fireball surface. They found that the time curve is affected by the curvature effect. When the background count is added (then the hardness ratio is called the raw hardness ratio), the curvature effect would bring about several types of the evolutionary curve, each type depending on the hardness of the bursts. The primary goal of this paper is to validate statistically the phenomena predicted by Qin et al. (2006). We try to check: a) If there indeed exist the three predicted types of the hardness ratio evolutionary curve when a sizable sample is examined; b) whether the hardness of the sources of the different types varied in the way (statistically speaking) predicted in Qin et al. (2006).

The selected GRB sample for our analysis is taken from Kocevski et al. (2003), which comprises 67 GRB sources with durations longer than 2 s. These sources are found to comprise 76 individual GRB pulses. These 67 GRB sources were all collected by the Burst and Transient Source Experiment (BATSE) on board the Compton Gamma-Ray Observatory (CGRO). These are FRED pulse sources and the profiles of the pulses were found to be in agreement with the expectation of the curvature effect (see Qin & Lu 2005).

The light curve data with the background counts subtracted are available in the BATSE website (<http://coss.gsfc.nasa.gov/docs/cgro/batse/batseburst/sixtyfour.ms/bckgnd.fits.html>). For one of the sources (#3259) no such data was given in the website, so reducing our sample to 66 sources. There are three double-peak sources and three triple-peak sources in the sample of Kocevski et al. (2003), and we chose only the first peak in each case for our analysis. The signal data are taken within the interval $[t_{\min}, t_{\max}]$, where $t_{\max} - t_{\min} = 2T_{90}$, and t_{\min} is at $T_{90}/2$ before the start of T_{90} .

Since the light curve function of Kocevski et al. (2003) (the KRL function) can well describe the observed profile of a FRED pulse, we simply adopted this function to fit the light curve of all bursts, where the parameters of the function are allowed to be different for different channels of the same burst. There are four free parameters in the KRL function, i.e., the maximum flux of the pulse F_m , the time of peak flux t_m , the power-law rise index r , and the power-law decay index d . In addition, we introduced a fifth parameter t_0 , which measures the offset between the start of the pulse and the trigger time. With the fifth parameter, the KRL function is expressed as:

$$F(t) = F_m \left(\frac{t - t_0}{t_m - t_0} \right)^r \left[\frac{d}{d+r} + \frac{r}{d+r} \left(\frac{t - t_0}{t_m - t_0} \right)^{(r+1)} \right]^{-\frac{r+d}{r+1}}, \quad (1)$$

which holds for $t \geq t_0$; for $t < t_0$ we take $F(t) = 0$.

3 HARDNESS RATIO CURVES

We use C_2 and C_3 to denote the observed counts of the second and third BATSE channels. The adopted C_2 and C_3 data are those with the background counts subtracted. The corresponding bi-channel light curve is defined as $C_{2+3} = C_2 + C_3$. Using a non-linear fit with the adopted KRL function, we obtain the peak of C_{2+3} , $C_{2+3,p}$. The corresponding time is denoted by t_m . By adding $C_{2+3,p}/2$ to C_2 and C_3 , we obtain new counts of the two BATSE channels, C'_2 and C'_3 . Then, the raw hardness ratio (RHR) can be written as (Qin et al. 2006)

$$\text{RHR} \equiv \frac{C'_3}{C'_2} = \frac{C_3 + \frac{C_{2+3,p}}{2}}{C_2 + \frac{C_{2+3,p}}{2}}, \quad (2)$$

with which we obtain the evolutionary curves of the Kocevski (2003) sample. Indeed, from a mere inspection of the profiles, we can classify the pulses into three groups: type 1 (3 sources), type 2 (40 sources), and type 3 (21 sources), only two sources could not be classified into any of these three types, which we assigned to type 4. The RHR curves of these four types are illustrated in Figures 1, 2, 3 and 4, respectively. We see that the type 1 sources exhibit a pulse-like profile without a dip in the decay phase; that the type 2 sources exhibit a pulse-like profile with a dip in the decay phase; and the type 3 sources exhibit an upside down phase. The raw hardness ratio curves of types 1 and 2 all possess a pulse-like profile and their peaks appear in advance of the corresponding light curves. These phenomena are consistent with the prediction made in Qin et al. (2006) (see the fourth panel of figs. 1–3 in Qin et al. 2006).

Using the software ORIGIN, we fit the curves of C_{2+3} and RHR for the Kocevski sample with the adopted KRL function, for which the fitting parameters as well as their uncertainties are available. The results of fitting are presented in Figures 1–4. The times of the maximum value (f_{m1}), and the minimum value (the dip marked with f_{m2}) are denoted by t_{m1} and t_{m2} , respectively and are obtained from the fitting. For type 1 sources, only f_{m1} and t_{m1} are available, while for type 3 sources, we have only f_{m2} and t_{m2} . These values along with t_m (for C_{2+3}), obtained from the fit with Equation (1), are listed in Table 1.

Qin et al. (2006) illustrated in the fourth panels of their figures 1–3 that very hard bursts possess in their raw hardness ratio curves a pulse-like profile without a dip in the decay phase (type 1), while hard sources have a pulse-like profile with a dip in the decay phase (type 2), and soft sources have a profile with only an upside down phase (type 3). This in turn suggests that type 1 sources should be very hard, type 2 sources should be hard, and type 3 sources should be soft. The hardness of a burst is defined as the ratio of its radiations of a higher energy band to a lower energy band. When using the BATSE data, the degree of the hardness of GRBs is generally denoted by the hardness ratio defined as the fluence of the third channel divided by the fluence of the second channel, and is denoted by HR. However, the term of “hardness” used in Qin et al. (2006) is slightly different. They used the peak energy E_p instead of the conventional hardness ratio. Adopting a rest frame Comptonized radiation with $\nu_{0,C} = 0.55 \text{ keV h}^{-1}$, Qin et al. (2006) used $\Gamma = 2000$ which corresponds to $E_p \sim 2500 \text{ keV}$ according to Qin (2002) to represent the typical very hard burst, and they used $\Gamma = 200$ ($E_p \sim 250 \text{ keV}$) and $\Gamma = 20$ ($E_p \sim 25 \text{ keV}$) to represent the typical hard and soft bursts, respectively. Since they adopted the same kind of rest frame spectrum with the same indexes in their analysis, each E_p used there corresponds to a single hardness ratio. To compare our results with their prediction, we should also use E_p . Unfortunately this cannot be done due to two reasons: a) the sample discussed here is composed of various sources which might be associated with different kinds of radiation mechanism and therefore a given E_p might correspond to different hardness ratios; b) the values of E_p are unavailable for our sample. Hence we cannot make a direct comparison between our analysis with the prediction made in Qin et al. (2006).

However, the idea that type 2 sources are softer than type 1 sources but harder than of type 3 sources can be checked with the conventional hardness ratio. If the prediction is wrong, then we would find that the hardness ratios of type 2 sources are generally smaller than that of type 3, or the distributions of the hardness ratio of the two types are not distinguishable. The data of the hardness ratio of BATSE sources are available from the same website ([/coss.c.gsfc.nasa.gov/docs/cgro/batse/4Bcatalog/4b_flux.html](http://coss.c.gsfc.nasa.gov/docs/cgro/batse/4Bcatalog/4b_flux.html)). In Figure 5, we show the HR distributions of the three groups of sources, as well as the small group of type 4 sources. It shows that, in terms of HR, sources of type 2 sources are indeed generally harder (their HR are generally larger) than those of type 3. A K-S test yields a null probability of $9.4E - 08$, which means that the fact that the HR values of type 2 sources are generally larger than those of type 3 sources is not due to random

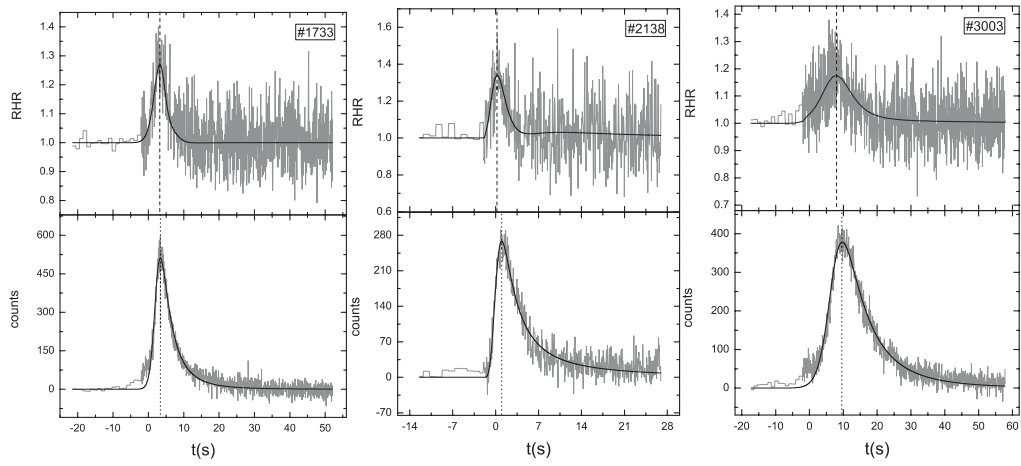


Fig. 1 Raw hardness ratio evolutionary curves (upper panels) and light curves (lower panels) of type 1 sources. The solid lines represent the best fits to the curves.

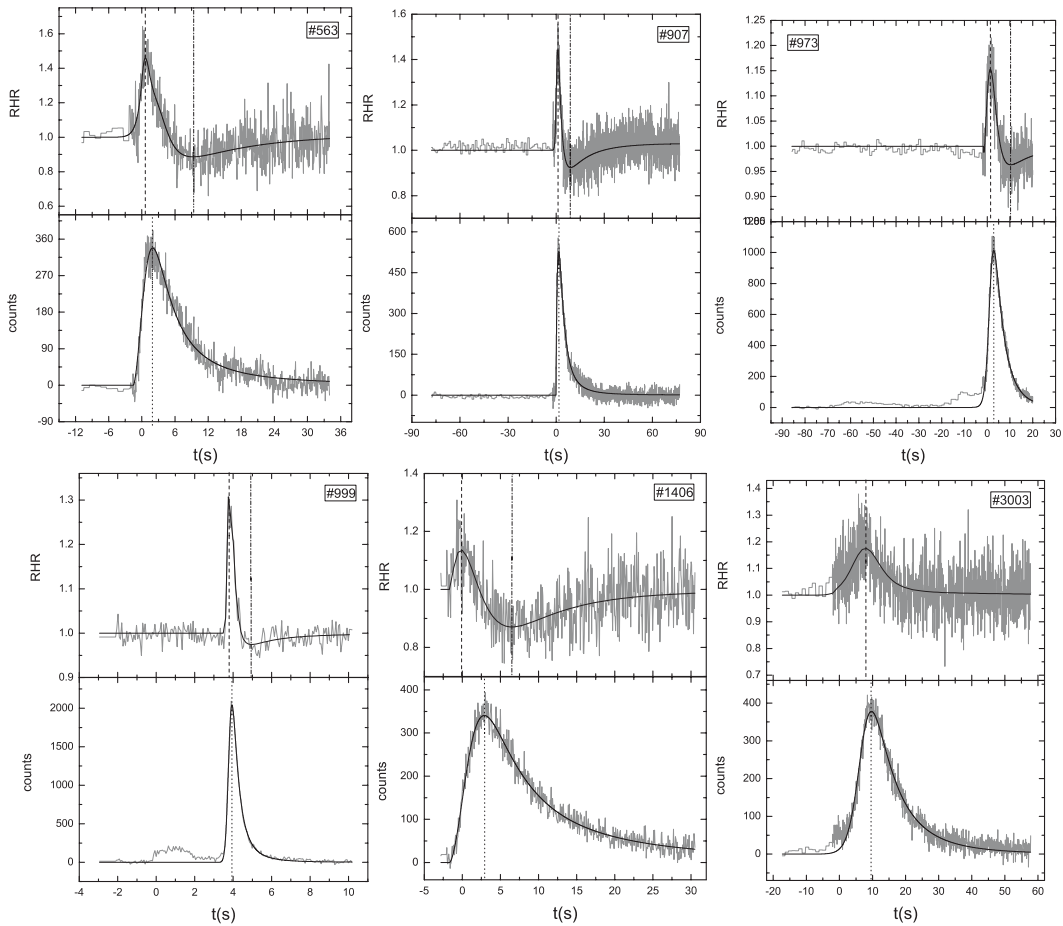


Fig. 2 Raw hardness ratio evolutionary curves (upper panels) and light curves (lower panels) of type 2 sources. The solid lines represent the best fits to the curves.

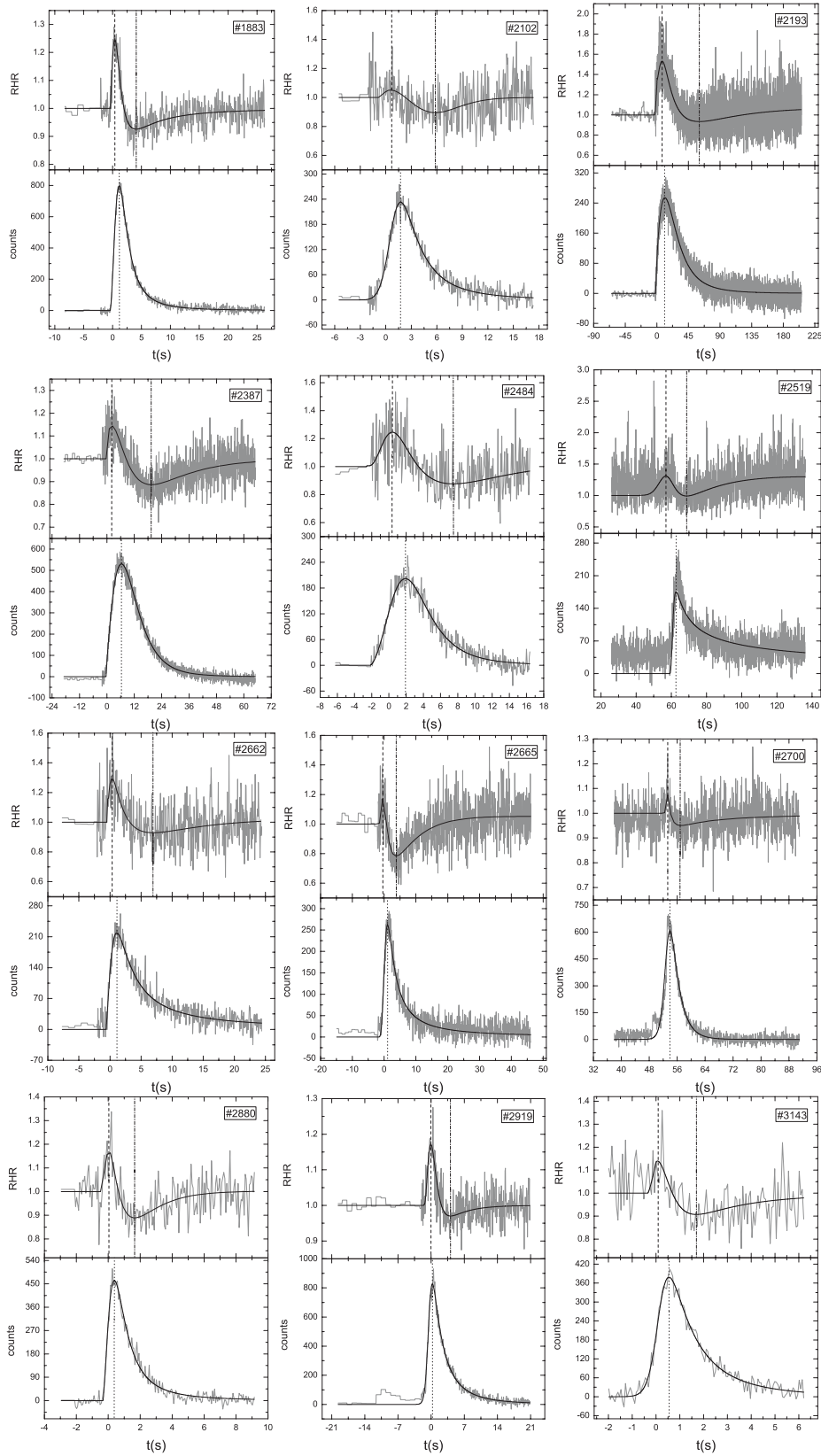


Fig.2 -Continued.

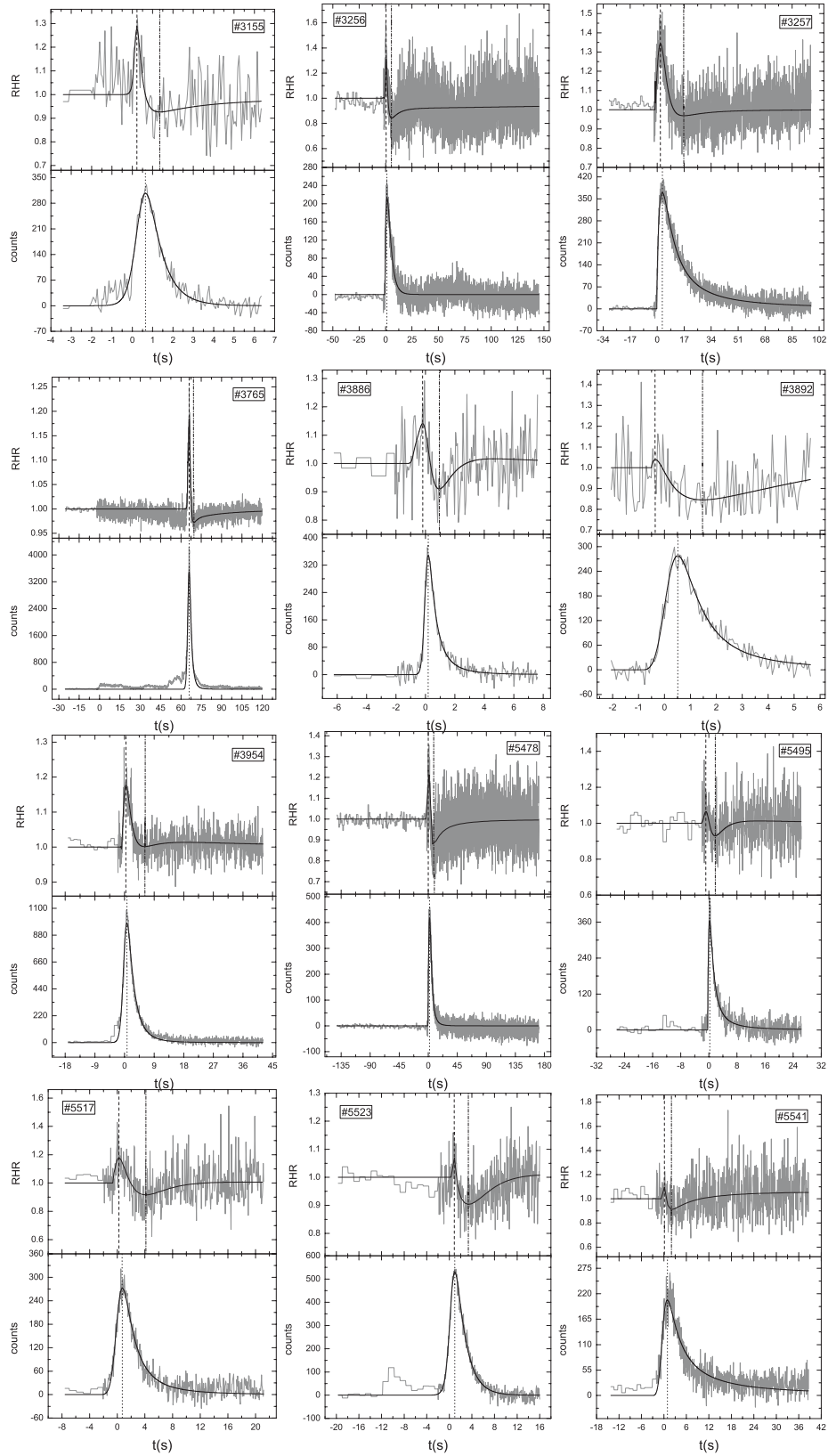


Fig. 2 -Continued.

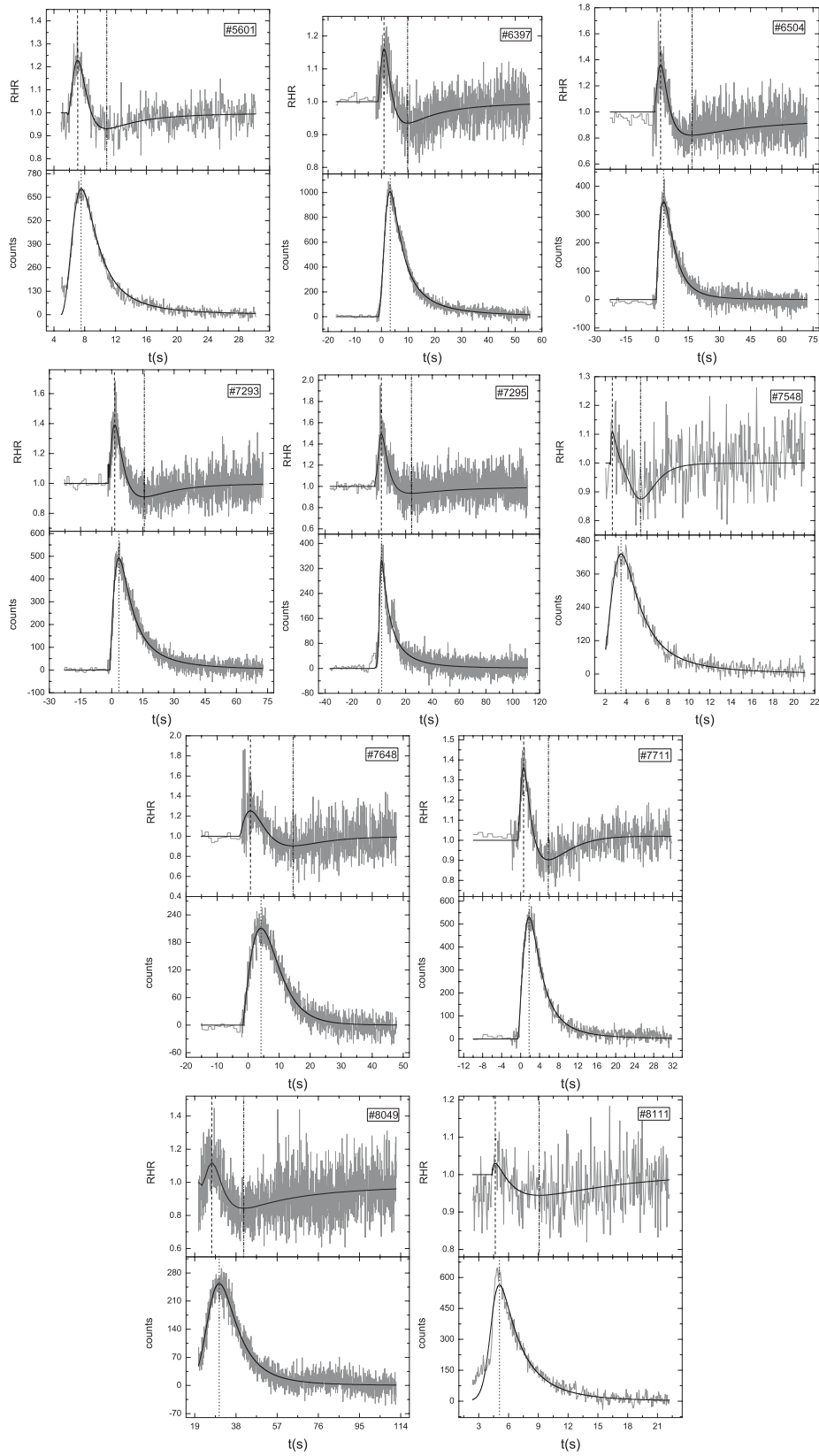


Fig. 2 - Continued.

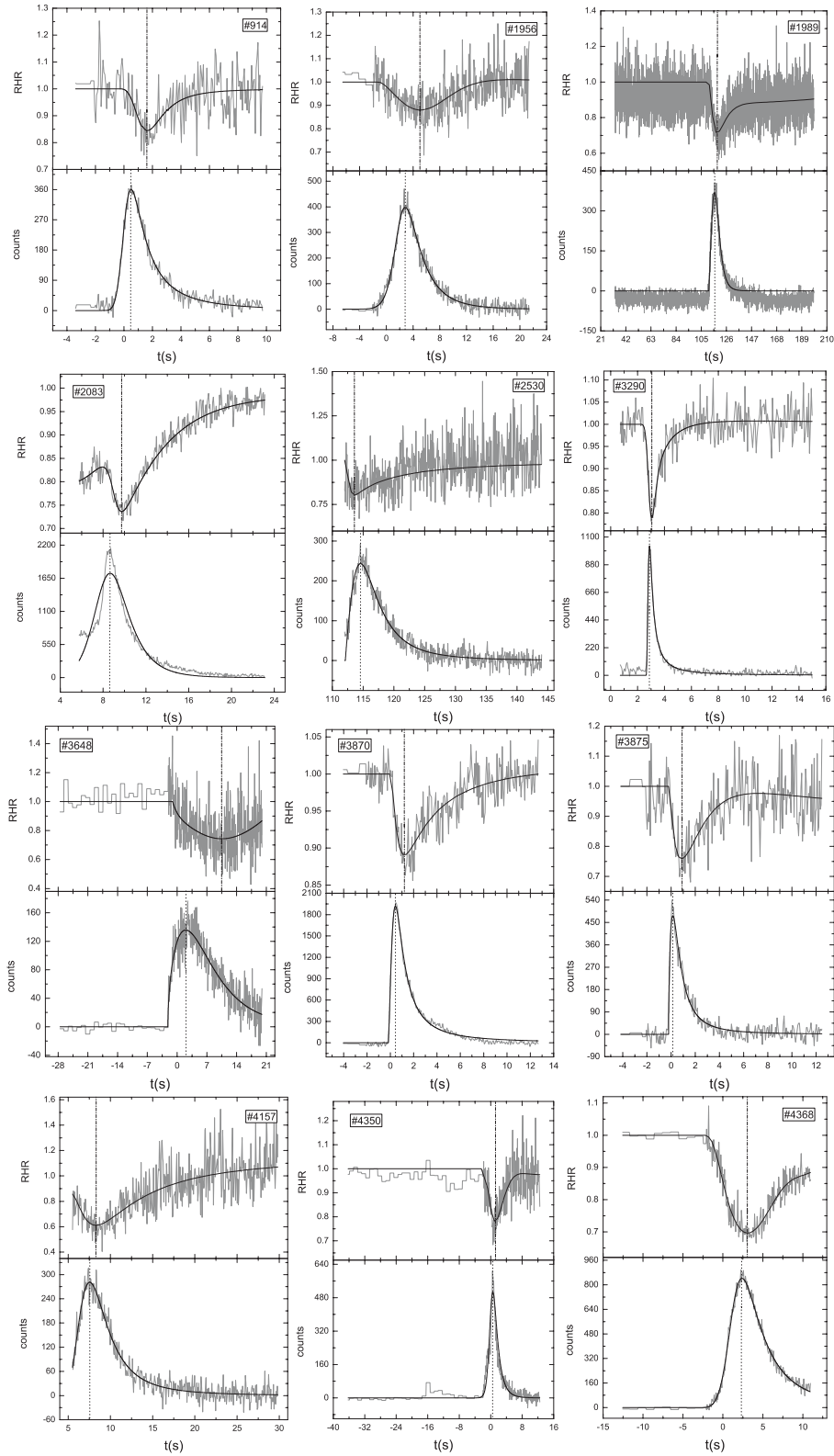


Fig. 3 Raw hardness ratio evolutionary curves (upper panels) and light curves (lower panels) of type 3 sources. The solid lines represent the best fits to the curves.

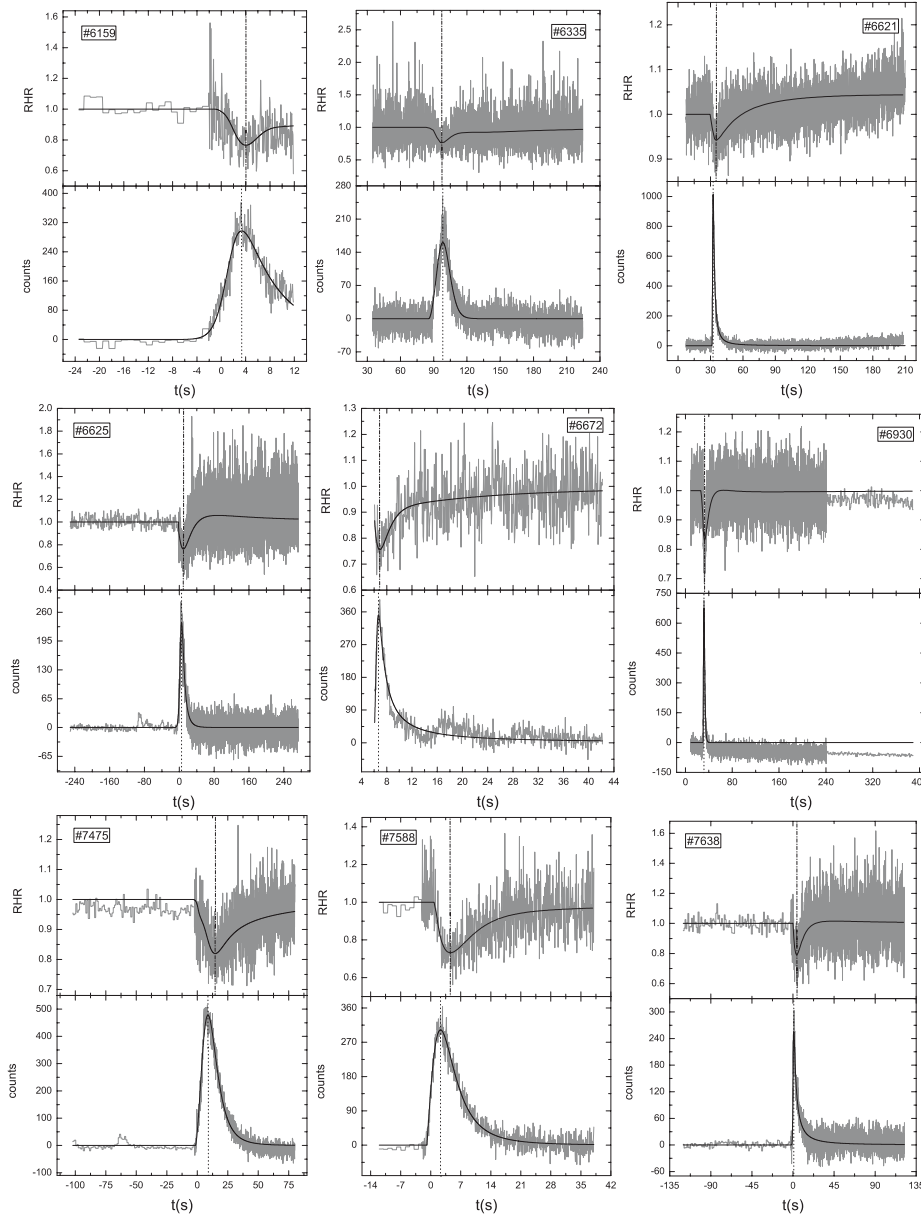


Fig. 3 -Continued.

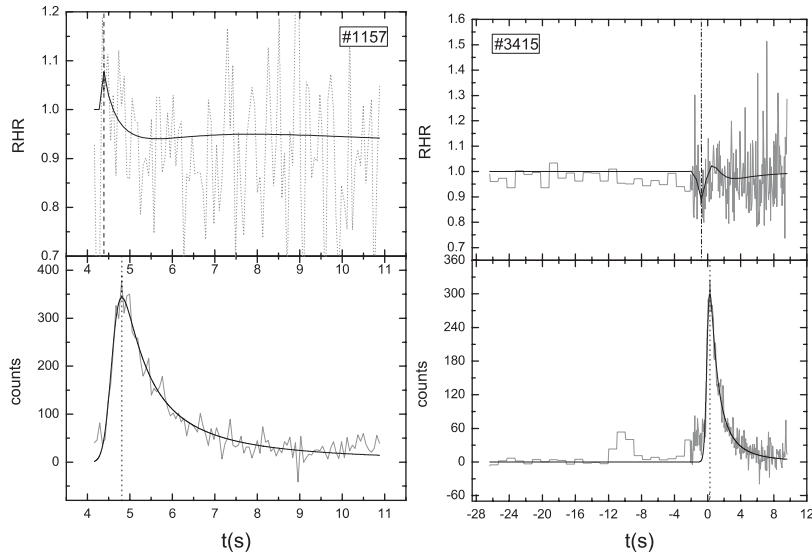
fluctuation. Since type 1 is represented by only three sources, we cannot perform a statistical analysis on the HR distribution. However, as Figure 5 shows, the sources of type 1 are indeed located in a harder domain.

In Figure 6, we present the distributions of Δt_1 , Δt_2 , f_{m1} and f_{m2} ($\Delta t_1 \equiv t_m - t_{m1}$ and $\Delta t_2 \equiv t_{m2} - t_m$). To examine whether these distributions are different for different types of sources, we carried out a K-S test. The resulting probabilities (that they are NOT different between types 2 and 3) are: $7.37E - 09$ for f_{m2} and $1.77E - 04$ for Δt_2 . Thus, it is indicated that type 2 and type 3 really differ from each other.

Figure 6 shows that f_{m2} could distinguish types 2 and 3 quite well. We suspect that for distinguishing the sources, the hardness ratio, f_{m2} , could be more sensitive than the conventional HR. See Figure 7. The plot confirms our suspicion by showing that, while the HR values of types 2 and 3 are overlap each other to a large extent, the degree of overlap in f_{m2} is much less.

Table 1 Estimated Parameters of the Three Types of Sources

Type	Trigger	t_{m1}	t_m	t_{m2}	f_{m1}	f_{m2}	Type	Trigger	t_{m1}	t_m	t_{m2}	f_{m1}	f_{m2}
1	1733	3.21	3.39	-	1.27	-	5541	0.18	0.87	2	1.1	0.91	
	2138	0.21	0.99	-	1.34	-	5601	7.03	7.47	10.9	1.23	0.93	
	3003	7.95	9.56	-	1.17	-	6397	0.97	3.16	9.72	1.16	0.93	
2	563	0.62	1.98	9.33	1.46	0.89	6504	1.9	3.14	16.7	1.36	0.82	
	907	1.45	2.13	8.81	1.44	0.92	7293	1.5	3.54	15.49	1.39	0.91	
	973	1.71	3.12	10.17	1.15	0.96	7295	1.82	2.47	24.49	1.49	0.94	
	999	3.79	3.95	4.91	1.31	0.97	7548	2.64	3.52	5.36	1.11	1	
	1406	-0.14	2.97	6.49	1.18	0.87	7648	0.72	4.28	14.44	1.25	0.9	
	1467	1.28	4.23	8.14	1.06	0.89	7711	0.52	1.78	5.9	1.36	1.02	
	1883	0.49	1.2	4.14	1.25	0.93	8049	26.98	30.11	41.5	1.12	0.84	
	2102	0.69	1.69	5.86	1.29	0.92	8111	4.64	5.07	9.1	1.03	0.94	
	2193	6.94	10.63	60.63	1.53	0.93	3	914	-	0.47	1.62	-	0.84
	2387	2.17	6.24	19.54	1.14	0.89	1956	-	2.88	5.02	-	0.88	
	2484	0.37	1.95	7.5	1.25	0.88	1989	-	116.31	118.45	-	0.72	
	2519	56.97	62.88	68.73	1.31	0.99	2083	-	8.61	9.71	-	0.74	
	2662	0.36	1.06	6.89	1.93	0.93	2530	-	114.6	113.64	-	0.8	
	2665	-0.39	0.97	3.67	1.17	1.05	3290	-	2.86	3.05	-	0.79	
	2700	53.33	53.82	56.76	1.11	0.95	3648	-	2.02	10.46	-	0.74	
	2880	0.03	0.35	1.68	1.17	0.89	3870	-	0.41	1.23	-	0.89	
	2919	0.01	0.2	4.13	1.17	0.97	3875	-	0.11	0.91	-	0.76	
	3143	0.1	0.53	1.71	1.14	0.91	4157	-	7.6	8.31	-	0.61	
	3155	0.21	0.67	1.35	1.28	0.93	4350	-	0.44	1.29	-	0.78	
	3256	0.23	1.01	5.13	1.31	0.84	4368	-	2.3	3.04	-	0.7	
	3257	2.06	3.14	16.75	1.34	0.97	6159	-	3.34	4.1	-	0.76	
	3765	65.9	65.9	69.66	1.18	0.97	6335	-	98.41	97.55	-	0.76	
	3886	-0.18	0.17	0.94	1.14	1.01	6621	-	32.54	35.13	-	0.94	
	3892	-0.37	0.5	1.47	1.04	0.85	6625	-	6.24	10.65	-	0.76	
	3954	0.42	0.67	6.37	1.18	1.01	6672	-	6.67	6.89	-	0.76	
	5478	0.71	1.99	8.69	1.25	0.88	6930	-	31.19	32.86	-	0.83	
	5495	-0.9	0.31	1.78	1.06	1.01	7475	-	8.8	15.03	-	0.82	
5517	0.25	0.75	4.15	2.09	1.01	7588	-	2.24	4.44	-	0.73		
5523	0.94	0.94	3.37	1.09	0.9	7638	-	1.29	4.41	-	0.79		

**Fig. 4** Raw hardness ratio evolutionary curves (upper panels) and the light curves (lower panels) of type 4 sources. The solid lines represent the best fits to the curves.

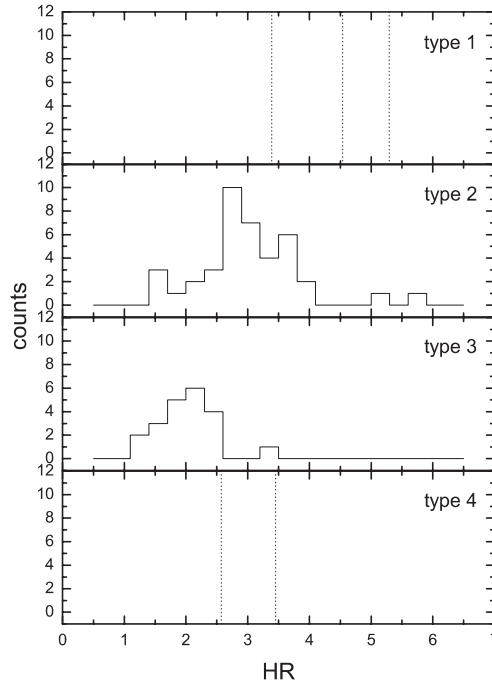


Fig. 5 Distributions of the conventional hardness ratio for sources of different types. The dotted lines stand for the position of HR of individual sources in types 1 and 4.

4 CONCLUSIONS

In this paper we concentrated on the time curve of the raw hardness ratio for a GRB sample. The raw hardness ratio is defined as the ratio of the counts of a higher to a lower energy channel, the counts including the background. Our sample contains 66 GRB sources given in Kocevski et al. (2003). We checked whether the prediction made in Qin et al. (2006) is true or not.

We found that there indeed exist three different types of profile in the raw hardness ratio evolutionary curve, as predicted in Qin et al. (2006): a) a pulse-like profile without a dip in the decay phase (type 1); b) a pulse-like profile with a dip in the decay phase (type 2); c) a profile with only an upside down phase (type 3). The peaks of the raw hardness ratio curves of types 1 and 2 indeed appear in advance of the corresponding light curves, which was also predicted in Qin et al. (2006). It was stated in Qin et al. (2006) that very hard, hard, and soft sources should have RHR profiles of types 1, 2, 3, respectively. Although we cannot directly check this result with the hardness parameter (E_p) used in Qin et al. (2006), we can test the prediction by using the conventional hardness ratio (HR). According to their analysis, if the prediction does not hold, then the HR distributions of types 2 and 3 will provide clues. Our analysis shows that, statistically, the sources of type 2 are indeed harder than sources of type 3 (the HR values are generally larger in type 2 than in type 3).

An additional finding comes from an analysis of the distribution of the minimum value of the RHR, f_{m2} : this is a much more sensitive parameter than the conventional hardness ratio HR for distinguishing the pulses of different types (see Fig. 7).

As seen in Figure 4, type 4 is unlikely a separate type. The failure of classifying the sources into any of the other three types must be due to poor data quality, with the signal associated with the harness ratio being too faint to be identified.

As mentioned above, the reason for adding the background count to the signal count is that we would like to see how the hardness ratio evolves within the period of a pulse, and by doing so the hardness ratio can be defined within smaller time intervals without degenerating into mere fluctuation. What would happen if we do not add a background count to the signal count? One might notice that the available signal data are observational counts free of the background counts (<http://coss.c.nasa.gov/doc/cgro/batse>

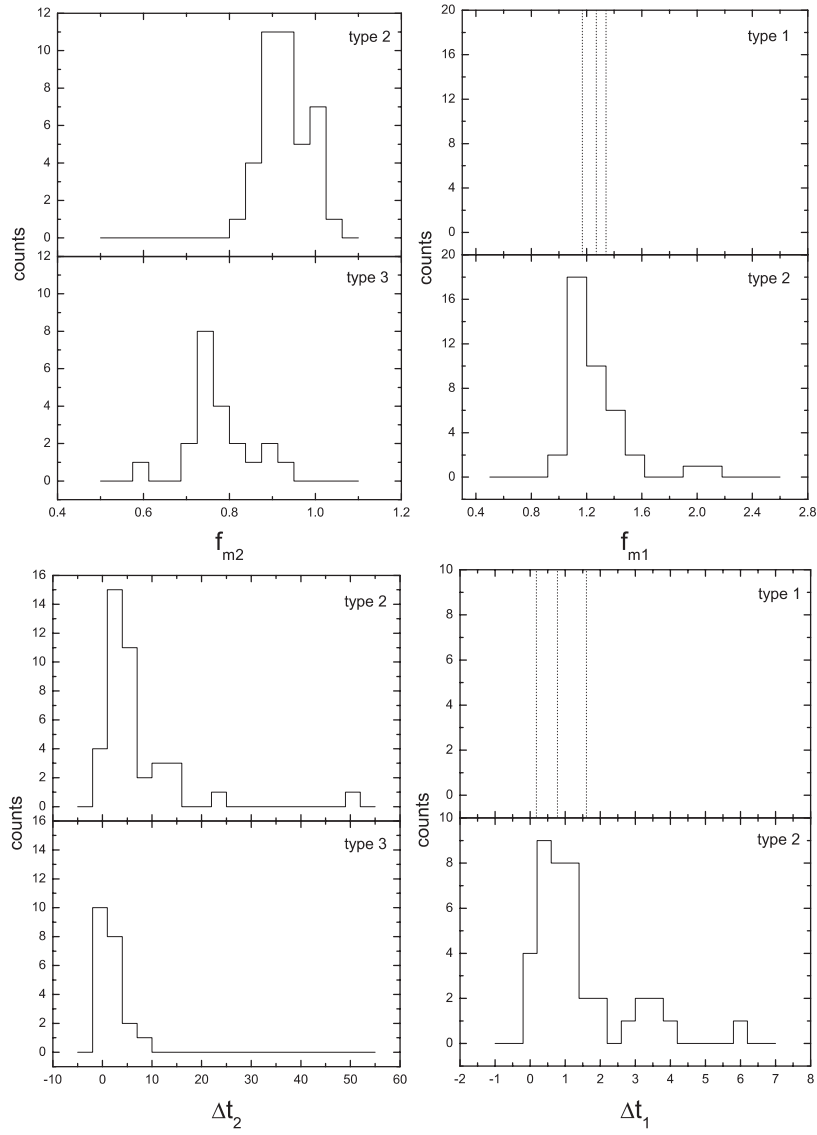


Fig. 6 Distributions for the maximum value f_{m1} and the minimum value f_{m2} of the RHR, and of Δt_1 and Δt_2 (defined in Sect. 3).

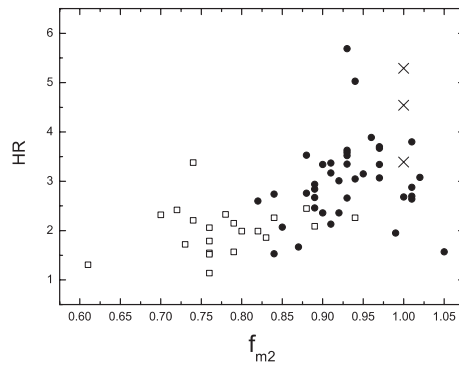


Fig. 7 A plot of f_{m2} vs. HR for types 1 (crosses), 2 (filled circles) and 3 (open squares). We put $f_{m2} = 1$ for type 1.

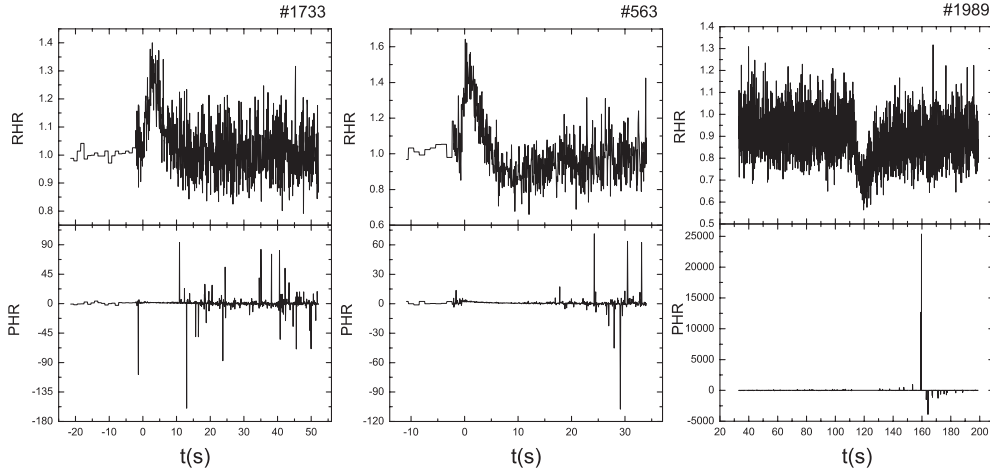


Fig. 8 Pure hardness ratio evolutionary curves (lower panels) for three typical sources #1733 (type 1), #563 (type 2) and #1989 (type 3). For comparison, the upper panels are the raw hardness ratio evolutionary curves.

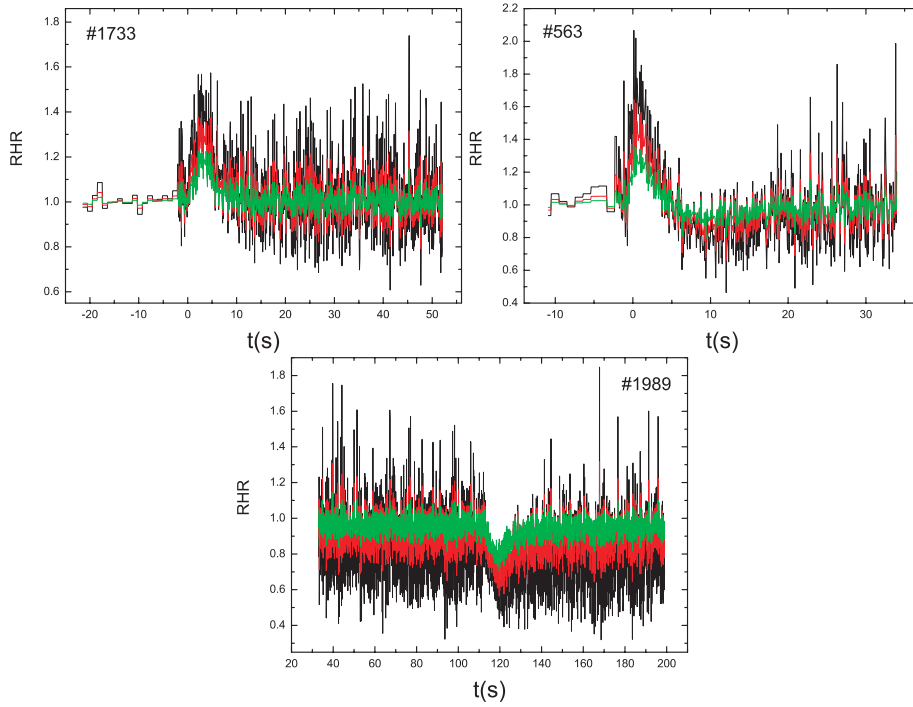


Fig. 9 Raw hardness ratio evolutionary curves for three typical sources #1733 (type 1), #563 (type 2) and #1989 (type 3), where the black, red and green colors stand for cases of adopting $C_{2+3,p}/4$, $C_{2+3,p}/2$ and $C_{2+3,p}$, respectively.

[/batseburst/sixtyfour_ms/bckgnd_fits.html](#)). As one can see from a plot of the counts, they are obviously affected by fluctuations. Thus we found negative values as well as zeros in the data sets. The value of C_3/C_2 would be infinity if $C_2 = 0$ and would be negative when either one is negative. In addition, when there are many datapoints of $C_2 \sim 0$, then the C_3/C_2 curve will show nothing but a chaos (even when the points of $C_2 = 0$ are excluded). Shown in Figure 8 are the pure hardness ratio evolutionary curves of three typical

bursts belonging to types 1, 2 and 3 respectively, calculated merely by subtracting the background counts (the $C_2 = 0$ points have been removed). The chaos shown in the figure must be due to fluctuation. This is the reason why we adopted the raw hardness ratio curve rather than the pure hardness ratio curve in our investigation.

As a certain background count is included in the definition of the raw hardness ratio (see Eq. (2)), what would one expect if a different background count is adopted? So we repeated the above analysis by replacing $C_{2+3,p}/2$ with $C_{2+3,p}$ and $C_{2+3,p}/4$, respectively. We found that the characteristics of the profiles of the RHR are maintained for either replacement. The classification of the sources into the three types is not affected. This can be expected since the replacement affects only a constant in both the numerator and denominator in Equation (2). The signal data are not affected. As expected, when $C_{2+3,p}$ is adopted, the signal characteristics become insignificant, while in the case of adopting $C_{2+3,p}/4$ the characteristics become more significant. At the same time, the chaos becomes less in the former case and greater in the latter case. Shown in Figure 9 are the corresponding plots of the RHR for the three typical bursts studied in Figure 8, after making the replacements.

According to the above analysis, we propose that the pulses of gamma-ray bursts may be divided into three groups according to the profile of their RHR curves or/and the minimum of RHR. Since the hardness of a pulse must be due to the strength of the shock or/and the magnetic field involved, pulses so divided would be helpful to connect the light curve with the underlying physical process.

Acknowledgements Thanks are due to the anonymous referee for helpful suggestion that significantly improved the paper. I also thank Dr. Alok C. Gupta for polishing up the English of the paper. This work is supported by the National Natural Science Foundation of China (Grants 10533050 and 10573030).

References

- Barthelmy S. D., Chincarini G., Burrows D. N. et al., 2005, *Nature*, 438, 994
 Borgonovo L., Ryde F., 2001, *ApJ*, 548, 770
 Burrows D. N., Romano P., Falcone A. et al., 2005, *Science*, 309, 1833
 Cusumano G., Mangano V., Chincarini G. et al., 2006, *Nature*, 440, 164
 Fenimore E. E., Madras C. D., Nayakshin S., 1996, *ApJ*, 473, 998
 Fox D. B., Frail D. A., Price P. A. et al., 2005, *Nature*, 437, 845
 Gehrels N., Chincarini G., Giommi P. et al., 2004, *ApJ*, 611, 1005
 Gehrels N., Sarazin C. L., O'Brien P. T. et al., 2005, *Nature*, 437, 851
 Goodman J., 1986, *ApJ*, 308, L47
 Hailey C. J., Harrison F. A., Mori K., 1999, *ApJ*, 520, L25
 Kargatis V. E., Liang E. P., BATSE Team, 1995, *Ap&SS*, 231, 177
 Kocevski D., Ryde F., Liang E., 2003, *ApJ*, 596, 389
 Lu R. J., Peng Z. Y., Dong W., 2007, *ApJ*, 663, 1110
 Meszaros P., Rees M. J., 1998, *ApJ*, 502, L105
 Norris J. P., Share G. H., Messina D. C. et al., 1986, *ApJ*, 301, 213
 Paczynski B., 1986, *ApJ*, 308, L43
 Qin Y. P., 2002, *A&A*, 396, 705
 Qin Y. P., 2003, *A&A*, 407, 393
 Qin Y. P., Zhang Z. B., Zhang F. W. et al., 2004, *ApJ*, 617, 439
 Qin Y. P., Lu R. J., 2005, *MNRAS*, 362, 1085
 Qin Y. P., Su C. Y., Fan J. H. et al., 2006, *Phys. Rev. D*, 74, 063005
 Roming P. W. A., Schady P., Fox D. B. et al., 2006, *ApJ*, 652, 1416
 Ryde F., Petrosian V., 2002, *ApJ*, 578, 290
 Ryde F., Svensson R., 2000, *ApJ*, 529, L13
 Ryde F., Svensson R., 2002, *ApJ*, 566, 210
 Tagliaferri G., Goad M., Chincarini G. et al., 2005, *Nature*, 436, 985